European Journal of Pharmaceutics and Biopharmaceutics 79 (2011) 232–240

Contents lists available at ScienceDirect

European Journal of Pharmaceutics and Biopharmaceutics

journal homepage: www.elsevier.com/locate/ejpb

Research paper

RGD-modified PEG–PAMAM–DOX conjugates: *In vitro* and *in vivo* studies for glioma

Lihong Zhang [a], Saijie Zhu [a], Lili Qian [a], Yuanying Pei [a], Yongming Qiu [b,*], Yanyan Jiang [a,*]

[a] Department of Pharmaceutics, Fudan Univeristy, Shanghai, China
[b] Department of Neurosurgery, Shanghai Jiaotong University, Shanghai, China

ARTICLE INFO

Article history:
Received 5 January 2011
Accepted in revised form 22 March 2011
Available online 8 April 2011

Keywords:
Poly(amidoamine) dendrimer
Poly(ethylene glycol)
RGD-peptide
Doxorubicin
Cellular uptake
Glioma

ABSTRACT

This work was based on our recent studies that a promising conjugate, RGD-modified PEGylated polyamidoamine (PAMAM) dendrimer with doxorubicin (DOX) conjugated by acid-sensitive *cis*-aconityl linkage (RGD-PPCD), could increase tumor targeting by binding with the integrin receptors overexpressed on tumor cells and control release of free DOX in weakly acidic lysosomes. To explore the application of RGD-PPCD to glioma therapy, the effects of the conjugate were further evaluated in glioma model. For comparative studies, DOX was also conjugated to PEG–PAMAM by acid-insensitive succinic linkage to produce the PPSD conjugates, which was further modified by RGD to form RGD-PPSD. *In vitro* cytotoxicity of the acid-sensitive conjugates against C6 cells was higher than that of the acid-insensitive ones, and further the modification of RGD enhanced the cytotoxicity of the DOX-polymer conjugates as a result of the increased cellular uptake of the RGD-modified conjugates by C6 cells. *In vivo* pharmacokinetics, biodistribution and antitumor activity were investigated in an orthotopic murine model of C6 glioma by i.v. administration of DOX-polymer conjugates. In comparison with DOX solution, all the conjugates showed significantly prolonged half-life and increased AUC and exhibited higher accumulation in brain tumor than normal brain tissue. Although RGD-PPCD was more than 2-fold lower tumor accumulation than RGD-PPSD, it exhibited the longest survival times among all treatment groups, and therefore, RGD-PPCD conjugate provide a desirable candidate for targeted therapy of glioma.

1. Introduction

Incidence of gliomas is approximately 5–10 per 100,000 population. Primary brain tumors are one of the 10 main causes of death by cancer [1]. The clinical application of chemotherapy to brain tumors has been limited because blood–brain barrier (BBB) prevents the uptake of all large-molecule and more than 98% of pharmaceutical and small-molecule drugs [2]. DOX, named as a strong candidate for chemotherapy of the central nervous system (CNS), has been shown to arrest cell growth and induce apoptosis in malignant glioma cell lines [3]. The improved survival of glioma patients by direct intratumoral infusion of DOX [4] and its efficacy against multiple cancer types point out the potential of DOX for clinical use against both primary and metastatic brain tumors if drug accumulation in the tumor could be increased to therapeutic levels [3]. However, DOX has seldom been effective in patients with brain tumors following systemic administration because of poor accumulation in glioma tissue [3,5].

Drug–polymer conjugates are potential candidates for the selective delivery of antitumor agents to tumor tissue. Poly(amidoamine) (PAMAM) dendrimers are highly branched, narrowly dispersed synthetic macromolecules with well-defined structure and composition. The unique structural features of PAMAM dendrimers make them ideal nanoplatforms to conjugate biologically important substances, drugs, targeting molecules, and imaging agents [6–8]. The branched architecture of dendrimers makes them particularly attractive for targeted delivery applications, as they can present targeting ligands in a manner favorable to promote multivalent binding to target cellular receptors [9].

The cell adhesion molecule integrin $\alpha_v\beta_3$ is particularly known for its role in cancer progression and is overexpressed in melanomas, glioblastoma, ovarian, breast, and prostate cancers. The Arg-Gly-Asp (RGD) containing peptides have been identified to have high affinity with integrin $\alpha_\upsilon\beta_3$ [10]. PAMAM–RGD conjugates have been found to mediate cellular binding and adhesion [9]. RGD-modified liposomes were able to enhance the intracellular uptake of the entrapped DOX by B16 melanoma tumor cells or human umbilical vein endothelial cells (HUVECs) and led to improved antitumor activity by the passive accumulation in tumor tissue and integrin-mediated endocytosis [11,12].

* Corresponding authors. Department of Neurosurgery, Renji Hospital, Shanghai Jiaotong University, School of Medicine, 1630 Dongfang Road. Shanghai 200127, China (Y. Qiu), Key Laboratory of Smart Drug Delivery, Ministry of Education & PLA, Department of Pharmaceutics, School of Pharmacy, Fudan Univeristy, 826 Zhangheng Road, Shanghai 201203, China (Y. Jiang). Tel.: +86 21 51980077; fax: +86 21 51980076.
E-mail addresses: qiuzhoub@hotmail.com (Y. Qiu), yanyanjiang@shmu.edu.cn (Y. Jiang).

0939-6411/$ - see front matter © 2011 Elsevier B.V. All rights reserved.
doi:10.1016/j.ejpb.2011.03.025

Incorporating acid-sensitive linkage between drugs and polymeric carriers is an attractive approach, which ensures effective release of the polymer-bound drug at the tumor site, while keeping the conjugates stable in the bloodstream [13–16]. In our previous reports, acid-sensitive *cis*-aconityl linkage or acid-insensitive succinic linkage was used to conjugate DOX to PEG–PAMAM to achieve PPCD or PPSD conjugate. We found that the acid-sensitive DOX release from PPCD conjugate ensured higher concentration of free DOX in tumor and more pronounced antitumor activity than the acid-insensitive PPSD conjugate [17,18]. With these promising results, PPCD was further modified by the cyclic pentapeptide RGDyC to produce the RGD-PPCD conjugate, which exhibited significantly improved therapeutic effect against murine B16 melanoma compared with PPCD [19].

Based on our recent studies, here, we are intended to explore the application of the targeted therapy of the RGD-PPCD conjugate to glioma. For comparative studies, the PPSD conjugate was also modified by RGD to produce the RGD-PPSD conjugate. The effect of RGD-peptide and drug linkage style on the cytotoxicity against C6 cells and cellular uptake was investigated. *In vivo* pharmacokinetic, biodistribution, and antitumor activity studies were further carried out to evaluate the passive targeting of DOX-polymer conjugates and the active targeting of RGD modification in an orthotopic murine C6 glioma model.

2. Materials and methods

2.1. Materials

PAMAM dendrimer generation 4 with an ethylenediamine core in methanol (10% w/v) was obtained from Dendritech, Inc. (Midland, MI, USA). Methoxy PEG Succinimidyl Carboxymethyl Ester with molecular weight of 5000 (MeO–PEG–SCM) and N-hydroxysulfosuccinimide-polyoxyethylene-maleimide (NHS–PEG–MAL, MW 5147) were purchased from JenKem Technology Co., Ltd. (Beijing, China). Cyclo (RGD–DTyr–C) was obtained from Chinese Peptide Co., (Hangzhou, China). 2-mercaptpethanol was purchased from Aladdin Reagent, Inc. (Shanghai, China). *Cis*-aconitic anhydride was obtained from Alfa Aesar (Lancashire, UK). Anhydrous DMF, trypan blue, *p*-dioxane, and succinic anhydride were purchased from Sinopharm Chemical Reagent Co., Ltd. (Shanghai, China). 3-(4,5-dimethylthiazol-2-yl)-2,5-diphenyl tetrazolium bromide (MTT) was obtained from Amresco (Solon, OH, USA). 1-ethyl-3-(3-dimethylaminopropyl) carbodiimide hydrochloride (EDC) was purchased from Shanghai Medpep Co., Ltd. (Shanghai, China). Doxorubicin Hydrochloride (DOX) was purchased from Zhejiang Hisun Pharmaceutical Co., Ltd. (Zhejiang, China). Male ICR mice (6–8 weeks old), ranging from 18 to 22 g, were provided by Sino-British Sippr/BK Laboratory Animal Co., Ltd. (Shanghai, China). All care and handling of animals were performed in accordance with the guidelines of the animal ethics committee of Fudan University (Shanghai, China).

2.2. Synthesis of RGD-modified PEG–PAMAM–DOX conjugates

2.2.1. Synthesis of PPCD and PPSD conjugates

The PEG–PAMAM–DOX conjugates with two DOX conjugation style, PPCD and PPSD conjugates, were synthesized according to our previous reports [17,18], respectively. Namely, PAMAM was first PEGylated with the feed molar ratio of PAMAM to MeO–PEG–SCM of 1:32, and then DOX was conjugated to the PEG–PAMAM conjugate by acid-sensitive cis-aconityl linkage and acid-insensitive succinic linkage to achieve PPCD and PPSD conjugates, respectively. The yields of PPCD and PPSD were 71.1% and 77.5% (percentage of the total amount of raw materials, PEG–PAMAM and DOX, W/W), respectively.

2.2.2. Synthesis of RGD–PEG–PAMAM–DOX conjugates

RGDyC was first conjugated to MAL–PEG–NHS by the reaction between the maleimide group of PEG and the thiol group of RGDyC [19]. Briefly, 4.0 mg of RGDyC (6.8 μmol) was dissolved in 1.5 ml of 0.1 M NaAc–HAc buffer (pH 6.0), and then 35 mg of MAL–PEG–NHS (6.8 μmol) were added and initiated the reaction by vortex mixing for 30 s. The above solution was added to PAMAM (2.15 mg, 0.15 μmol) in 1.5 ml of 0.05 M borate buffer (pH 9.2) (RGD:PEG:-PAMAM = 45:45:1, molar ratio). The reaction mixtures were stirred at room temperature for 24 h. Then, pH of the above reaction mixtures was adjusted to 7.0 by 1 M HCl, and 4.8 μl of 2-mercaptpethanol was added to quench the unreacted maleimide group. After another 1 h of reaction at room temperature, the reaction mixture was placed in an ultrafiltration tube (Millipore, USA, MWCO 30,000) and centrifuged at 5000 rpm for 30 min for 5–6 times. Thin layer chromatography (TLC) was used to monitor the purity of the products until no PEG could be detected in the upper solution (chloroform/methanol/water = 1/1/0.1, v/v/v). The products were retrieved by freeze drying from the aqueous solution and white solids were obtained. The yield of RGD–PEG–PAMAM was 59.5% (percentage of the total amount of raw materials, PAMAM, PEG, and RGDyC, W/W).

Cis-aconityl-doxorubicin (CAD) was synthesized using the method previously reported [17] before preparing RGD–PEG–PAMAM–*cis*-aconityl–DOX conjugate (RGD-PPCD). CAD was conjugated to the RGD–PEG–PAMAM conjugates in the presence of water-soluble carbodiimide EDC at room temperature in the dark [20]. Briefly, CAD (56 mg, 74.7 μmol) and EDC (153 mg, 746.7 μmol) were dissolved in 25 ml of 0.2 M phosphate buffer (pH 6.0) and stirred at room temperature in the dark. After 30 min, RGD–PEG–PAMAM conjugate in 3 ml of distilled water (CAD: RGD–PEG–PAMAM = 100:1, molar ratio) was added, and pH value of the reaction mixture was adjusted to 8.0 by 0.5 M NaOH. The reaction mixture was then left to react in the dark for 12 h. Unreacted CAD and other small-molecules were separated from the conjugate on a Sephadex G-25 fine column (3.6 × 55 cm) eluted with phosphate buffered saline (pH 7.4). The macromolecular fractions of RGD-PPCD conjugates were collected, ultrafiltrated, dialyzed against distilled water, and lyophilized to obtain red solids. The yield of RGD-PPCD was 68.4% (percentage of the total amount of raw materials, RGD–PEG–PAMAM and CAD, W/W).

To prepare RGD–PEG–PAMAM–succinic–DOX conjugate (RGD-PPSD), DOX was first converted to its succinic anhydride derivative (SAD), and then the active ester of SAD (SAD–NHS) was obtained by the reaction between SAD and NHS [17,18]. RGD-PPSD conjugates were prepared by coupling of RGD–PEG–PAMAM–NH_2 and SAD–NHS. Namely, the reaction mixture of SAD–NHS was added to RGD–PEG–PAMAM conjugate in phosphate buffer (pH 8.0) (SAD: RGD–PEG–PAMAM = 50:1, molar ratio), with the pH adjusted to 8.0 by 1 M HCl. After 12 h of reaction at room temperature, the reaction mixture was dialyzed against distilled water to remove DMF, and small molecular substances were separated from the conjugate on a Sephadex G-25 fine column (3.6 × 55 cm) eluted with PBS (pH 7.4). The macromolecular fractions of RGD-PPSD conjugates were collected, ultrafiltrated, dialyzed against distilled water, and lyophilized to obtain red solids. The yield of RGD-PPSD was 74.5% (percentage of the total amount of raw materials, RGD–PEG–PAMAM and SAD, W/W).

2.3. Characterization of conjugates

^{1}H-NMR spectra of the synthesized conjugates were recorded on a Mercury Plus 400 MHz spectrometer (Bruker, Germany). Particle size was determined by dynamic light scattering (Malvern Instruments Ltd., UK). DOX content (wt.%) in each conjugate was

quantified by hydrolyzing the glycosidic bond between the doxorubicinone and amino sugar at acidic condition and determining the released doxorubicinone using HPLC [17,18]. Then, the conjugated number of DOX per PAMAM dendrimer was obtained.

2.4. In vitro cytotoxicity

C6 glioma cells were purchased from Institute of Biochemistry and Cell Biology (IBCB), Shanghai Institutes for Biological Sciences, Chinese Academy of Sciences (Shanghai, China) and cultured in the DMEM medium supplemented with 10% FBS, antibiotics (penicillin 80 U/ml, streptomycin 80 μg/ml), and incubated in the incubator at 37 °C in humidified environment of 5.0% CO_2 (THERMO CO_2 incubator). C6 cells were seeded at a density of 1×10^4 cells/well in 96-well transparent plate and incubated for 24 h. The medium was then replaced by PAMAM, PEG–PAMAM, RGD–PEG–PAMAM, free DOX, or DOX-polymer conjugates. The tested concentration ranges were 0–100 μM PAMAM-equiv. for PAMAM and PAMAM conjugates, and 0–600 μM DOX-equiv. for free DOX and DOX-polymer conjugates. The cell viability was determined by the MTT assay. After incubation for 60 h, the medium was removed, and the wells were washed twice with PBS. 10% MTT (5 mg/ml in PBS) in medium was added, and the cells were incubated for 4 h. After that, the medium was removed, and 100 μl dimethylsulfoxide (DMSO) was added. The plate was agitated for 10 min, and then, each well was finally analyzed by the microplate reader with absorbance detection at 570 nm. The IC_{50} values were expressed as concentration (μM) of PAMAM dendrimer-equiv. or DOX-equiv.

2.5. Cellular uptake

C6 cells were seeded in 6-well transparent plate at a density of 2.5×10^5 cells/ml (1-ml cell suspension per well) and incubated for 24 h. DOX-polymer conjugates containing 60 μM DOX-equiv. in serum-free culture media were added, and the cells were incubated for 60 min at 37 °C. After incubation, conjugate solutions were removed, and the cells were washed three times with ice-cold PBS (pH 7.4). Thereafter, to detach the cells from the dishes (37 °C, 3.5 min), 0.5 ml of 0.25% trypsin-0.05% EDTA solution was added. Extracellular fluorescence was quenched by trypan blue (0.25% in PBS pH 7.4) for 5 min at room temperature [20]. Finally, the cells resuspended in PBS were subjected to fluorescence-activated cell sorting analysis. For the determination of total cellular fluorescence, the procedure of trypan blue quenching was omitted.

Cell-associated fluorescence was analyzed using a Becton Dickinson FACSCalibur cytometer (San Jose, CA, USA) equipped with an argon laser (488 nm) and emission filter for 550 nm. Data collection involved 10,000 counts per sample. The data were analyzed using CELLQuest™ software and expressed as the geometric mean of the entire population. Cells incubated without DOX-polymer conjugates were used to account for the background fluorescence.

2.6. Pharmacokinetic and biodistribution in brain tumor–bearing mice

ICR mice were anesthetized intraperitoneal (i.p.) with 10% Chloral Hydrate (400 mg/kg) and then immobilized on a stereotactic holder (Stoeling 51700, USA). After the skull was exposed, a hole was made 2.0 mm lateral (right) to the midline, as measured from the *Bregma*. The 10^5 C6 cells suspended in 3 μl DMEM (free of serum) were injected slowly into the brain with a Hamilton syringe at a 3-mm depth. A waiting time of 3–5 min was implemented after injection to prevent reflux. Three to five minutes after the injection had finished, the syringe was slowly removed, the scission site closed with suture silk (5.0), and the animal left to recover in a warm environment (about 25 °C).

Brain tumor–bearing mice were allowed to grow for approximately 2 weeks. The DOX solution or DOX-polymer conjugates was injected intravenously via tail veil at a dose of 7.5 mg DOX-equiv./kg body weight. At the desired times, blood was collected from retro-orbital sinus after ether anesthesia and centrifuged (3000 rpm, 10 min) to isolate the plasma. Mice were immediately sacrificed by cervical dislocation, and their tissues (brain, tumor, heart, spleen, lung, kidney, and liver) were collected, washed with cold saline, dried over filter paper, weighed, and frozen at −20 °C until analysis.

Determination of total DOX was performed after acid hydrolysis to release doxorubicinone from polymer-bound DOX followed by HPLC separation.

2.7. Efficacy studies

The antitumor efficacy of the DOX-polymer conjugates was evaluated in ICR mice harboring a brain tumor. Orthotopic glioma animal models were made as described above. Treatments were given at 24 h postinoculation and consisted of four kinds of DOX-polymer conjugates (a dose of 7.5 mg DOX-equiv./kg body weight), saline, and DOX saline solution (a dose of 7.5 mg/kg body weight) as the negative and positive control, respectively. The drug was given by intravenous injection via tail vein on every 7 day for four times (days 1, 7, 14, and 21) [21]. Mice were then checked for survival every day.

2.8. Data analysis

Data are expressed as mean ± standard deviations (SD). Significant differences in the mean values were evaluated by Student's *t*-test. Places needing multiple comparisons were evaluated by one-way ANOVA with Boferroni correction. *P* value of 0.05 or less was considered to be statistically significant. Pharmacokinetic modeling and pharmacokinetic parameter estimations were carried out using pharmacokinetic software 3P97 (Mathematics Institute, Academy of Science, Beijing, China). Survival curves were built on the basis of a Kaplan–Meier curve, and their statistical differences were determined using a log-rank (Mantel–Cox) test. Differences between mean values were considered significant when $p < 0.05$.

3. Results

3.1. Synthesis and characterization of DOX-polymer conjugates

PPCD, PPSD, and RGD-PPCD conjugates were synthesized, respectively, using our previously reported methods [17–19] with some minor modifications. In addition, the acid-insensitive RGD-PPSD conjugate was also prepared in this study. Unbond CAD/SAD as impurities of the DOX-polymer conjugates evaluated using GPC was less than 0.6% (mol.), which was similar to our previous report. The conjugates were characterized by ^{1}H-NMR spectrum. The PEGylation degree and the number of RGD attached to PAMAM were estimated using the proton integration method, by taking the characteristic peaks of PEG, RGD, and PAMAM into account (Fig. 1). The results listed in Table 1 were almost consistent with our previous reports [17–19]. About 19 molecules of PEG and 10 molecules of RGD were attached to one molecule of PAMAM dendrimer. DOX was then conjugated to RGD–PEG–PAMAM via acid-sensitive or acid-insensitive linkage. The number of conjugated DOX molecule per RGD–PEG–PAMAM conjugate was around 13. The size of four conjugates was approached to each other at the range of about 17–20 nm, which was close to our previously synthesized conjugates.

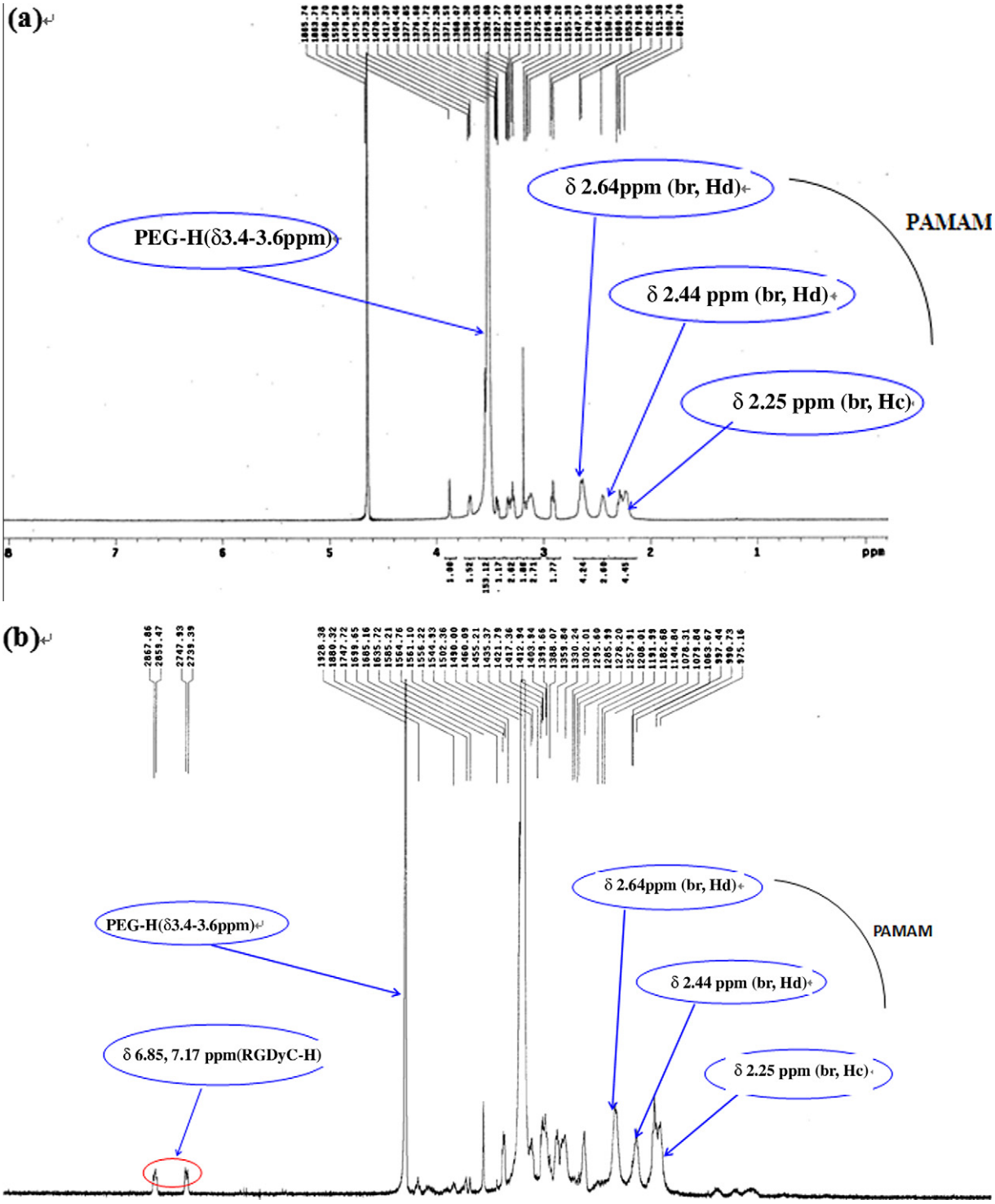

Fig. 1. ^{1}H-NMR spectra of PEG–PAMAM (a) and RGD–PEG–PAMAM (b) in D_2O. (For interpretation of the references to colour in this figure legend, the reader is referred to the web version of this article.)

3.2. In vitro cytotoxicity

Fig. 2a shows the viability of C6 cells after 60 h of incubation with PAMAM dendrimer, PEG–PAMAM, and RGD–PEG–PAMAM conjugates. Similar to our previous studies [18,22], G4 PAMAM dendrimer was indeed cytotoxic against C6 cells with the IC_{50} value of 2.06 μM, while the modification of PEG remarkably reduced the cytotoxicity of PAMAM even that the IC_{50} values of PEG–PAMAM could not be calculated owing to more than 50% of cells still alive at the highest concentration. However, the significant difference of cytotoxicity between PEG–PAMAM and RGD–PEG–PAMAM was observed in Fig. 2a, though the IC_{50} values of RGD–PEG–PAMAM could not also be obtained within experimental concentration range. Therefore, RGD–PEG–PAMAM conjugate exhibited higher

Table 1
Characteristics of DOX-polymer conjugates.

Conjugates	Conjugated number per PMAMA			Estimated M.W. kDa (n = 3)	Size (nm) (n = 3)
	DOX	PEG	RGDyC		
PPCD	12.9	18.9	–	119.71	18.72 ± 0.78
PPSD	12.7	18.9	–	106.60	17.81 ± 0.79
RGD-PPCD	12.6	19.0	10.1	126.07	20.23 ± 0.74
RGD-PPSD	13.5	19.0	10.1	126.59	19.99 ± 0.92

Conjugated number per PMAMA: The numbers of RGDyC, PEG mean the relative amount of them which was calculated by ^{1}H-NMR spectra using the proton integration method. The numbers of DOX per PMAMA were converted from DOX content (wt.%) in DOX-polymer conjugates.
Estimated M.W.: Being calculated by taking the numbers of DOX, RGDyC, PEG, and PAMAM into account.

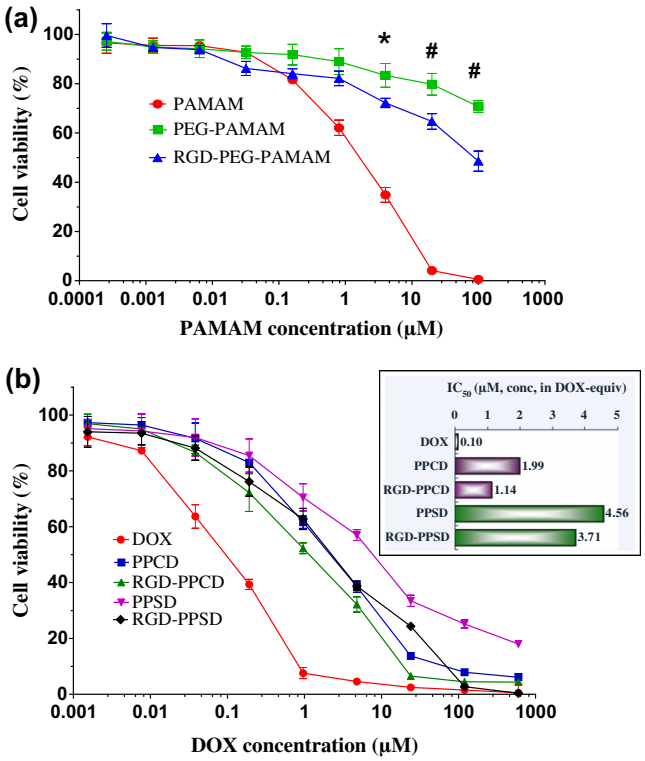

Fig. 2. In vitro cytotoxicity against C6 cells after 60 h of incubation. (a) PAMAM dendrimer and the modified PAMAM conjugates, $^*P < 0.05$; $^\#P < 0.01$, as compared with PEG–PAMAM at the same concentration; (b) DOX, PPCD, RGD-PPCD, PPSD, and RGD-PPSD conjugates (insert: IC_{50} values of free DOX and the DOX-polymer conjugates after 60 h of incubation). Data were expressed as mean ± standard deviation (n = 3). (For interpretation of the references to colour in this figure legend, the reader is referred to the web version of this article.)

cytotoxicity than PEG–PAMAM conjugate. The possible reason was that RGD-peptide has a capability to induce apoptosis [23].

The cytotoxicities of the DOX-polymer conjugates against C6 cells were evaluated and compared with free DOX. Fig. 2b shows the viability of C6 cells after 60 h of incubation with DOX and DOX-polymer conjugates, and an insert in Fig. 2b displays the IC_{50} values. All the four DOX-polymer conjugates showed much lower cytotoxicity as compared with free DOX. The IC_{50} values of acid-sensitive DOX-polymer conjugates were lower than that of acid-insensitive ones. RGD-modified conjugates displayed lower IC_{50} values than the unmodified ones. As a result, RGD-PPCD conjugate showed the highest cytotoxicity against C6 glioma cells compared with the other three.

3.3. Cellular uptake

Fig. 3 displays the internalized and total fluorescence of C6 cells after incubation with DOX-polymer conjugates (60 μM DOX-equiv.). It was found that both total and internalized fluorescence intensity of free DOX were much higher than those of any of DOX-polymer conjugate ($P < 0.01$). The total fluorescence intensity of the acid-insensitive conjugates (PPSD and RGD-PPSD) was greater than that of the acid-sensitive conjugates (PPCD and RGD-PPCD) (PPSD vs. PPCD, $P < 0.01$; RGD-PPSD vs. RGD-PPCD, $P < 0.05$). Furthermore, both total cellular uptake and internalization of the RGD-modified conjugates were significantly higher than those of the RGD-unmodified ones ($P < 0.05$), suggesting that RGDyC played a positive role in the cellular uptake of the DOX-polymer conjugates (Fig. 3).

3.4. In vivo pharmacokinetics

The DOX plasma concentration–time curves after intravenous injection of DOX solution and DOX-polymer conjugates are presented in Fig. 4. As seen in the figure, after injection of DOX solution, free DOX was quickly removed from the circulating system. In contrast, DOX-polymer conjugates exhibited markedly delayed blood clearance. The concentration–time curve for DOX solution and DOX-polymer conjugates were fitted by three-compartment and two-compartment model, respectively. The major pharmacokinetic parameters are shown in Table 2. All the DOX-polymer conjugates showed significantly altered pharmacokinetic parameters compared with DOX solution. The main pharmacokinetic parameters, including $T_{1/2\beta}$, MRT, and AUC, varied as follows: PPSD > RGD-PPSD > PPCD > RGD-PPCD > DOX. Coupling of DOX to PEG-PAMAM and RGD–PEG–PAMAM conjugates significantly prolonged elimination half-life ($T_{1/2\beta}$) and mean residence time (MRT) of DOX. Both central volume of distribution (Vc) and total body clearance (Cl)

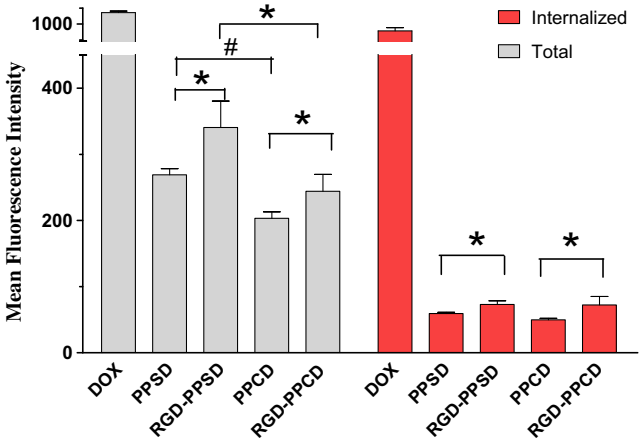

Fig. 3. Total cellular uptake and internalization of free DOX and DOX-polymer conjugates (60 μM DOX-equiv.) by C6 cells at 37 °C for 1 h. Data were expressed as mean ± standard deviation (n = 3). $^*P < 0.05$; $^\#P < 0.01$. (For interpretation of the references to colour in this figure legend, the reader is referred to the web version of this article.)

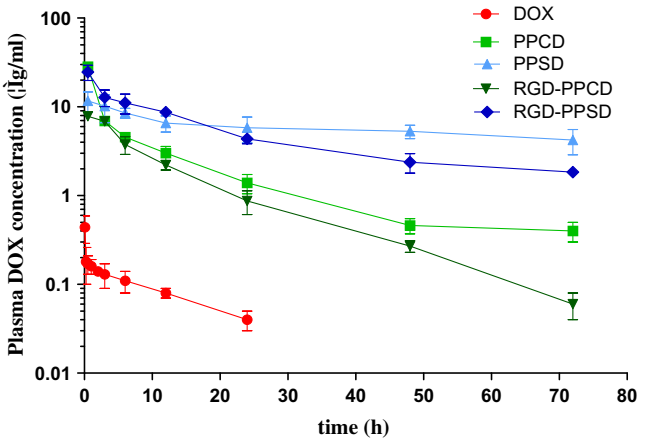

Fig. 4. Pharmacokinetic profiles in the orthotopic glioma-bearing mice after, i.v. administration of DOX solution and DOX-polymer conjugates at a dose of 7.5 mg DOX-equiv./kg ($n = 4$). (For interpretation of the references to colour in this figure legend, the reader is referred to the web version of this article.)

Table 2
Pharmacokinetic parameters of DOX in the orthotopic glioma-bearing mice after, i.v. administration of DOX solution or DOX-polymer conjugates at a dose of 7.5 mg DOX-equiv./kg ($n = 4$).

Group	AUC (hμg/ml)	$T_{1/2\beta}$ (h)	Vc (ml/kg)	Cl (ml/h/kg)	MRT (h)
DOX	2.17	12.37	3364.69	2614.45	8.87
PPCD	154.15	16.64	739.57	50.53	13.04
RGD-PPCD	92.42	14.29	855.99	85.88	12.35
PPSD	429.47	71.12	303.82	11.80	31.56
RGD-PPSD	363.16	62.40	388.91	18.96	20.62

AUC: Area under the plasma DOX concentration–time curves ($0 \rightarrow tn$).
$T_{1/2\beta}$: Elimination half-life.
Vc: Central volume of distribution.
Cl: Total body clearance.
MRT: Mean residence time.

were dramatically reduced accordingly. Correspondingly, AUC of DOX was also increased by 42.6-, 71.0-, 167.4-, and 197.9-fold for RGD-PPCD, PPCD, RGD-PPSD, and PPSD, respectively. The acid-insensitive conjugates showed greater AUC, $T_{1/2\beta}$, and MRT and less Vc and Cl than the acid-sensitive ones. AUC, $T_{1/2\beta}$, and MRT of the RGD-modified DOX-polymer conjugates decreased, Vc and Cl increased compared with that of the RGD-unmodified ones. The results indicated that both the drug conjugation style and RGD modification had major effects on the pharmacokinetic profile of DOX-polymer conjugates.

3.5. In vivo biodistribution of DOX-polymer conjugates

Following i.v. administration of free or DOX-polymer conjugates at a dose of 7.5 mg DOX-equiv./kg, biodistribution was examined in mice bearing orthotopic C6 brain tumors. Fig. 5 shows DOX deposition in brain tumor, normal brain tissue, liver, spleen, heart, lung, and kidney. The calculated AUC values in tumor and normal tissues are summarized in Table 3. Obviously, the accumulation of all the conjugates as well as free drug in brain normal tissue was extremely low compared with other tissues, which similar results was reported by Arnold et al. [24]. However, the DOX-polymer conjugates showed the changed tissue distribution characteristic and increased tumor accumulation tendency. Peak tumor concentrations ($C_{max,t}$) of 3.4–11.5 μg/g tumor observed at 12–24 h after i.v. injection of the conjugates were significantly higher than that of free drug (2.9 μg/g tumor

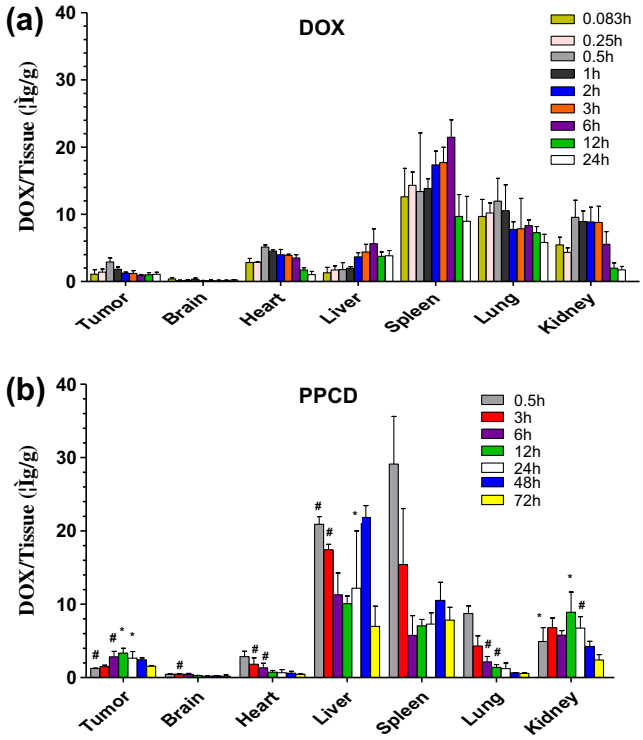

Fig. 5. Distribution profiles of total DOX in tissues after intravenous administration of DOX-polymer conjugates (over 72 h) and DOX solution (over 24 h). (a) DOX,(b) PPCD, (c) PPSD, (d) RGD-PPCD, and (e) RGD-PPSD at a dose of 7.5 mg DOX-equiv./kg ($n = 4$). $^{*}P < 0.05$; $^{\#}P < 0.01$, as compared with DOX solution at the same time point. (For interpretation of the references to colour in this figure legend, the reader is referred to the web version of this article.)

at 0.5 h, $P < 0.05$ vs. PPCD, and $P < 0.01$ vs. RGD-PPCD, PPSD or RGD-PPSD). Among these conjugates, $C_{max,t}$ of PPSD was higher than that of PPCD, while that of RGD-modified conjugates were higher than non-modified ones. Correspondingly, the AUC values of DOX in tumor for PPCD, RGD-PPCD, PPSD, and RGD-PPSD were 5.6-, 8.0-, 16.5-, and 21.2-fold higher than that of free drug, respectively. Furthermore, the tumor deposition of all conjugates was higher than normal tissues except liver and spleen, and the accumulation of DOX-polymer conjugates in spleen was extremely high, especially RGD-PPCD.

3.6. Efficacy studies

Survival of C6 glioma-bearing mice after different treatments was presented in a Kaplan–Meier plot as indicated in Fig. 6, and the differences among survival curves were compared using the log-rank test. There were a few animals survival in PPSD (1 mouse), RGD-PPSD (4 mice), and RGD-PPCD (5 mice) groups at day 84 after orthotopic implantation. Animals treated with saline had a median survival time of 17 days (Table 4). Animals treated with free DOX (Median: 14 days) or PPCD conjugate (Median: 16 days) had no statistically significant difference compared to saline group ($P > 0.05$). RGD-PPCD, RGD-PPSD, and PPSD conjugates were found to be significantly more effective in prolonging mice survival than DOX solution ($P < 0.01$). Particularly, animals treated with RGD-PPCD demonstrated a significant prolonged survival compared to PPCD ($P < 0.01$). Moreover, median ILS over saline group and ILS over DOX group of RGD-PPCD increased to 47.1 days and 50th day, 175.4% and 248.9%, indicating that RGD-PPCD exhibited the most effective in prolonging mice survival.

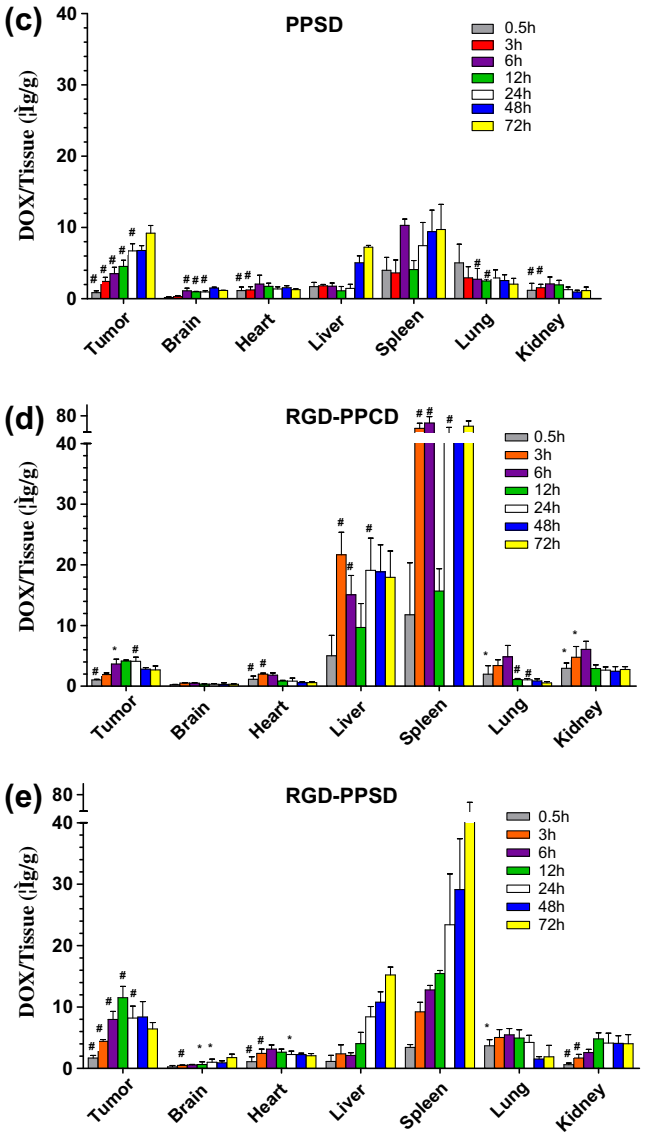

Fig. 5 (*continued*)

Table 3
AUC values of total DOX in various tissues of mice after i.v. injection of DOX solution or DOX-polymer conjugates at a dose of 7.5 mg DOX-equiv./kg.

Group	Tissue $AUC_{0\rightarrow tn}$ (h μg/g)						
	Tumor	Brain	Heart	Liver	Spleen	Lung	Kidney
DOX	24.80	4.27	55.38	97.15	309.70	176.50	91.31
PPCD	173.10	17.87	53.19	1043.00	646.60	89.26	383.20
RGD-PPCD	234.10	23.80	58.39	1232.00	3138.00	89.89	210.20
PPSD	458.20	78.26	107.60	260.60	574.60	187.40	92.60
RGD-PPSD	579.90	64.30	165.50	646.60	1927.00	223.70	280.70

4. Discussion

Therapy of malignant glioma remains very difficult for the aggressive growth and impossibility of complete surgical excision. Additionally, the existence of BBB, even if partially destroyed, still hinders the effective drug location in tumor tissue. Meanwhile, intracranial antitumor agent delivery would result in unexpected side effects. One strategy for circumventing the toxicity associated with chemotherapy is selective targeting of antitumor agents to the tumor site while sparing surrounding healthy tissue. It is well established that RGD sequence is present in many extracellular

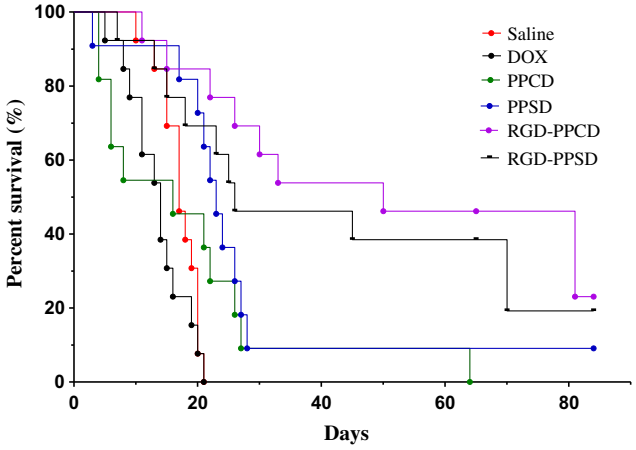

Fig. 6. *In vivo* effects of DOX solution and DOX-polymer conjugates after intravenous administration at a dose of 7.5 mg DOX-equiv./kg on the survival of brain tumor–bearing ICR mice. Saline, DOX, RGD-PPCD, and RGD-PPSD: $n = 13$; PPCD and PPSD: $n = 11$. (For interpretation of the references to colour in this figure legend, the reader is referred to the web version of this article.)

matrix components and can bind to α_v-integrins. The α_v-integrins are overexpressed on brain tumor cells and sprouting endothelial cells, but not on normal brain cells and quiescent endothelial cells, and constitute an attractive target for brain tumor imaging and therapy [25].

Our previous work had demonstrated that DOX release from PPCD conjugates followed an acid-triggered manner and increased from pH 7.4 (<5% at 96 h) to pH 4.5 (>60% at 96 h), which covered the pH condition from plasma to lysosome [17]. In contrast, PPSD conjugates released negligible amount of DOX (less than 1.0%) over 96 h at any pH condition [17,18]. Moreover, RGD modification did not vary the release behavior of the DOX-polymer conjugates [19]. PPCD exhibited higher *in vitro* and *in vivo* antitumor activity than PPSD in SKOV-3 ovarian carcinoma model or B16 murine melanoma model [17,18]. C6 cells may be similar to HUVEC and B16 cells that the free DOX released from acid-sensitive DOX-polymer conjugates in the acidic cellular organelles after internalization diffused into the nucleus subsequently to induce cells apoptosis[19]. It was further confirmed that the RGD modification enhanced significantly tumor uptake and showed higher antitumor efficacy than PPCD, indicating the active targeting ability of RGD-PPCD [19]. In this study, the advantages of the acid-sensitive RGD-PPCD conjugate used in the treatment of glioma included 2 aspects: ① increase in the antitumor efficacy by the ability of passive and active targeting of the drug specifically to the tumor site and ② control release of free DOX in weakly acidic lysosomes to ensure the lower free drug exposure in normal tissue and the higher cytotoxicity against tumor cells.

In vitro, DOX had the highest uptake by C6 glioma cells compared with the DOX-polymer conjugates and thus showed much strong cytotoxicity with the IC_{50} value of 0.1 μM against C6 cells, which was in the same magnitude with the results of our previous reports (0.23 μM against SKOV-3 cells [18] and 0.24 μM against B16 cells [17]). While in the intracranial C6 model, DOX is not effective that probably attributes to the existence of BBB and short blood circulation time. The total fluorescence intensity of PPSD conjugates was higher than that of PPCD conjugates. From our prior studies, the possible reasons is that the more positive charge on the surface of PPSD conjugates promoted their interaction with cells. Moreover, the uptake amount of RGD-modified conjugates was higher than that of RGD-unmodified ones because of the ligand-receptor-specific interaction. The result led to the higher cytotoxicity of RGD-PPSD or RGD-PPCD than that of PPSD or PPCD. Importantly, although no significant difference was found between

Table 4
Effects of various DOX formulations treatment on the survival of C6 brain tumor–bearing ICR mice (Saline, DOX, RGD-PPCD and RGD-PPSD: $n = 13$, PPCD and PPSD: $n = 11$).

Group	Median (days)	ILS over saline group (%)	ILS over DOX group (%)	*P* value
Saline	17	–	–	–
DOX	14	−21.1	–	>0.05 vs. saline
PPCD	16	8.8	37.8	>0.05 vs. saline
PPSD	23	56.7	98.5	0.0042 vs. saline
RGD-PPSD	26	134.5	197.0	0.0018 vs. saline; >0.05 vs. PPSD
RGD-PPCD	50	175.4	248.9	<0.0001 vs. saline; 0.0011 vs. PPCD

Median: The median survival.
ILS: Increase in life span ($((T/C - 1) \times 100$ (%)), where T and C represent the mean survival time (days) of the treated and control animals, respectively.
P **values**-were calculated by using the log-rank (Mantel–Cox) test.

the internalized intensity of the acid-sensitive and the acid-insensitive conjugates, the acid-sensitive PPCD or RGD-PPCD conjugate showed higher cytotoxicity than the acid-insentitive PPSD or RGD-PPSD conjugate. This result could be explained by acid-sensitive release of DOX after cellular uptake. DOX was reported to cause cell cycle arrest by the initiation of DNA damage through several proposed mechanisms that required the presence of drug in the nucleus and direct interaction with genomic DNA [26]. According to our previous study [17,18], DOX-polymer conjugates were delivered to lysosomes, where the slightly acidic condition permitted the release of DOX from PPCD conjugates and the subsequent entrance into nuclei, which was essential for cytotoxicity. However, PPSD conjugates released no free DOX to enter into nuclei, thus were less cytotoxic. Taking into account the results of cellular uptake, cytotoxicity, and intracellular localization according to our previous study [17,18], the acid-sensitive release of DOX was found to play an important role in determining the cytotoxicity of the DOX-polymer conjugates.

In vivo pharmacokinetic and biodistribution studies were performed to further explore the feasibility of RGD-modified PEG-PAMAM as the carrier of DOX for brain tumor targeting. The obtained results have demonstrated the long circulation and tumor targeting ability of the polymeric delivery system. DOX-polymer conjugates prolonged the circulation time of drug. PPSD conjugates displayed longer circulation time, less reticuloendothelial system (RES) uptake, and higher tumor accumulation than PPCD conjugates. The main reasons would be that PPSD conjugates had higher surface positive charge and were more hydrophobic [17]. On the other hand, the RGD modification shortened the circulation time of DOX-polymer conjugates. The phenomenon was consistent with other reports [27–29] and our recent study in subcutaneous B16 mice model [19]. For the present study of the biodistribution in intracranially implanted C6 glioma model, there was a difference from our previous studies in subcutaneous SKOV-3 nude mice and B16 mice model [17,18]. It was significantly different deposition of drug in the brain, that is, there was certain drug amount to be determined for all treatment groups in the brain of C6 glioma-bearing mice (whether in tumor tissue or in normal brain tissue). While the DOX content in brain was seldom detected in subcutaneously implanted tumor models. The most possible reason was the disruption of localized BBB in intracranial glioma animals led to increase BBB permeability. It was worthy of note that the total DOX deposition in heart, an organ of cumulative DOX toxicity, had no significant difference between the PPCD conjugates and the DOX solution, indicating less free drug in heart following the treatment of acid-sensitive conjugates. In addition, the accumulation of RGD-modified DOX-polymer conjugates in the spleen of intracranial glioma animals was much higher than those unmodified ones. The result was similar to other reports [24,27–29]. The reason is maybe similar to the report by Xiong et al. [27]. In the spleen, RGD-modified conjugates were probably associated with macrophages. Macrophages express α_v-integrins, using them to sequester and remove apoptotic cells from the circulation. It is likely that α_v-mediated uptake by macrophages in the spleen is also responsible for the uptake of RGD-modified conjugates. RGD-modified conjugates showed shorter circulation time and higher AUC values in spleen compared with unmodified ones, which demonstrated that modification of RGD-peptide resulted in an increased accumulation of the modified conjugates in spleen. Therefore, the spleen is probably responsible for the enhanced clearance of RGD-modified conjugates from the circulation.

In efficacy studies, systemic administration of PPCD and DOX solution at a dose of 7.5 mg/kg showed no significantly different therapeutic effects compared with saline ($P > 0.05$). The possible reason was that the tumor uptake of DOX for DOX solution was little, much shorter circulation time, and the increased accumulation of free DOX in heart, which is most sensitive to DOX toxicity. PPCD also showed no therapeutic effect that may be due to the lowest tumor accumulation among all the DOX-polymer conjugates resulting in inadequate effective level of free drug in the tumor site. Although the tumor accumulation of RGD-PPSD conjugate was markedly higher than that of RGD-PPCD, it was found that the administration of RGD-PPCD led to significant improvement in the median survival time of brain tumor-bearing animals (median: RGD-PPCD 50 days vs. RGD-PPSD 26 days). This result was consistent with that of *in vitro* studies (cytotoxicity and cellular uptake) and also could be explained by acid-sensitive release of free DOX after uptake of tumor cells.

5. Conclusions

A series of DOX-polymer conjugates with one PEGyaltion degree and different drug conjugation style: PPCD, PPSD, RGD-PPCD, and RGD-PPSD were evaluated *in vitro* and *in vivo* glioma models. RGD modification and drug conjugation style were found to affect the *in vitro* cytotoxicity, cellular uptake, *in vivo* biodistribution, and antitumor activity. Our results of studies proved RGD-PPCD showed the highest cytotoxicity *in vitro* and significant treatment efficacy *in vivo* compared with other conjugates, RGD-PPCD might be a potential candidate for targeted therapy of glioma and worthy of further investigation.

Acknowledgements

This work was supported by the National Basic Research Program of China (973 Program, 2007CB935802), National Science and Technology Major Project (2009ZX09310-006), Science and Technology Commission of Shanghai Municipality (0952nm03900) and Key Discipline Project of Renji Hospital (Shanghai Jiaotong University School of Medicine, RJ 4101307).

References

[1] X. Ying, H. Wen, W.L. Lu, J. Du, J. Guo, W. Tian, Y. Men, Y. Zhang, R.J. Li, T.Y. Yang, D.W. Shang, J.N. Lou, L.R. Zhang, Q. Zhang, Dual-targeting daunorubicin liposomes improve the therapeutic efficacy of brain glioma in animals, Journal of Controlled Release 141 (2010) 183–192.
[2] W.M. Pardridge, BBB-genomics: creating new openings for brain-drug targeting, Drug Discovery Today 6 (2001) 381–383.
[3] L.H. Treat, N. McDannold, N. Vykhodtseva, Y.Z. Zhang, K. Tam, K. Hynynen, Targeted delivery of doxorubicin to the rat brain at therapeutic levels using MRI-guided focused ultrasound, International Journal of Cancer 121 (2007) 901–907.

[4] K.A. Walter, R.J. Tamargo, A. Olivi, P.C. Burger, H. Brem, Intratumoral chemotherapy, Neurosurgery 37 (1995) 1128–1145.
[5] H. Vonholst, E. Knochenhauer, H. Blomgren, V.P. Collins, L. Ehn, M. Lindquist, G. Noren, C. Peterson, Uptake of adriamycin in tumour and surrounding brain-tissue in patients with malignant gliomas, Acta Neurochirurgica 104 (1990) 13–16.
[6] S.M. Moghimi, A.C. Hunter, J.C. Murray, Nanomedicine: current status and future prospects, Faseb Journal 19 (2005) 311–330.
[7] I.J. Majoros, T.P. Thomas, C.B. Mehta, J.R. Baker, Poly(amidoamine) dendrimer-based multifunctional engineered nanodevice for cancer therapy, Journal of Medicinal Chemistry 48 (2005) 5892–5899.
[8] A.K. Patri, A. Myc, J. Beals, T.P. Thomas, N.H. Bander, J.R. Baker, Synthesis and in vitro testing of J591 antibody–dendrimer conjugates for targeted prostate cancer therapy, Bioconjugate Chemistry 15 (2004) 1174–1181.
[9] C.L. Waite, C.M. Roth, PAMAM–RGD conjugates enhance siRNA delivery through a multicellular spheroid model of malignant glioma, Bioconjugate Chemistry 20 (2009) 1908–1916.
[10] Q. Li, W. Xu, Novel anticancer targets and drug discovery in post genomic age, Current Medicinal Chemistry – Anti-Cancer Agents 5 (2005) 53–63.
[11] X.B. Xiong, Y. Huang, W.L. Lu, X. Zhang, H. Zhang, T. Nagai, Q. Zhang, Enhanced intracellular delivery and improved antitumor efficacy of doxorubicin by sterically stabilized liposomes modified with a synthetic RGD mimetic, Journal of Controlled Release 107 (2005) 262–275.
[12] Y.F. Zhang, J.C. Wang, D.Y. Bian, X. Zhang, Q. Zhang, Targeted delivery of RGD-modified liposomes encapsulating both combretastatin A-4 and doxorubicin for tumor therapy: in vitro and in vivo studies, European Journal of Pharmaceutics and Biopharmaceutics 74 (2010) 467–473.
[13] W.C. Shen, H.J.P. Ryser, cis-Aconityl spacer between daunomycin and macromolecular carriers: a model of pH-sensitive linkage releasing drug from a lysosomotropic conjugate, Biochemical and Biophysical Research Communications 102 (1981) 1048–1054.
[14] P. Chytil, T. Etrych, C. Konak, M. Sirova, T. Mrkvan, B. Rihova, K. Ulbrich, Properties of HPMA copolymer–doxorubicin conjugates with pH-controlled activation: effect of polymer chain modification, Journal of Controlled Release 115 (2006) 26–36.
[15] A. Kakinoki, Y. Kaneo, Y. Ikeda, T. Tanaka, K. Fujita, Synthesis of poly(vinyl alcohol)–doxorubicin conjugates containing cis-aconityl acid-cleavable bond and its isomer dependent doxorubicin release, Biological and Pharmaceutical Bulletin 31 (2008) 103–110.
[16] H.S. Yoo, E.A. Lee, T.G. Park, Doxorubicin-conjugated biodegradable polymeric micelles having acid-cleavable linkages, Journal of Controlled Release 82 (2002) 17–27.
[17] S.J. Zhu, M.H. Hong, G.T. Tang, L.L. Qian, J.Y. Lin, Y.Y. Jiang, Y.Y. Pei, Partly PEGylated polyamidoamine dendrimer for tumor-selective targeting of doxorubic, in: The effects of PEGylation degree and drug conjugation style, Biomaterials 31 (2010) 1360–1371.
[18] S.J. Zhu, M.H. Hong, L.H. Zhang, G.T. Tang, Y.Y. Jiang, Y.Y. Pei, PEGylated PAMAM dendrimer–doxorubicin conjugates: in vitro evaluation and in vivo tumor accumulation, Pharmaceutical Research 27 (2010) 161–174.
[19] S.J. Zhu, L.L. Qian, L.H. Zhang, Y.Y. Pei, Y.Y. Jiang, RGD-modified PEG–PAMAM–DOX conjugate: in vitro and in vivo targeting to both tumor neovascular endothelial cells and tumor cells, Advanced Materials (in press).
[20] D. Raucher, A. Chilkoti, Enhanced uptake of a thermally responsive polypeptide by tumor cells in response to its hyperthermia-mediated phase transition, Cancer Research 61 (2001) 7163–7170.
[21] V. Kansara, D. Paturi, S.H. Luo, R. Gaudana, A.K. Mitra, Folic acid transport via high affinity carrier-mediated system in human retinoblastoma cells, International Journal of Pharmaceutics 355 (2008) 210–219.
[22] Y.Y. Jiang, G.T. Tang, L.H. Zhang, S.Y. Kong, S.J. Zhu, Y.Y. Pei, PEGylated PAMAM dendrimers as a potential drug delivery carrier: in vitro and in vivo comparative evaluation of covalently conjugated drug and noncovalent drug inclusion complex, Journal of Drug Targeting 18 (2010) 389–403.
[23] M.S. Aguzzi, P. Fortugno, C. Giampietri, G. Ragone, M.C. Capogrossi, A. Facchiano, Intracellular targets of RGDS peptide in melanoma cells, Molecular Cancer 9 (2010) (Article No.: 84).
[24] R.D. Arnold, D.E. Mager, J.E. Slack, R.M. Straubinger, Effect of repetitive administration of doxorubicin-containing liposomes on plasma pharmacokinetics and drug biodistribution in a rat brain tumor model, Clinical Cancer Research 11 (2005) 8856–8865.
[25] C.Y. Zhan, B. Gu, C. Xie, J. Li, Y. Liu, W.Y. Lu, Cyclic RGD conjugated poly(ethylene glycol)-co-poly(lactic acid) micelle enhances paclitaxel anti-glioblastoma effect, Journal of Controlled Release 143 (2010) 136–142.
[26] D.A. Gewirtz, A critical evaluation of the mechanisms of action proposed for the antitumor effects of the anthracycline antibiotics adriamycin and daunorubicin, Biochemical Pharmacology 57 (1999) 727–741.
[27] X.B. Xiong, Y. Huang, W.L. Lu, X. Zhang, H. Zhang, T. Nagai, Q. Zhang, Intracellular delivery of doxorubicin with RGD-modified sterically stabilized liposomes for an improved antitumor efficacy: in vitro and in vivo, Journal of Pharmaceutical Sciences 94 (2005) 1782–1793.
[28] A.J. Schraa, R.J. Kok, H.E. Moorlag, E.J. Bos, J.H. Proost, D.K.F. Meijer, L. de Leu, G. Molema, Targeting of RGD-modified proteins to tumor vasculature: a pharmacokinetic and cellular distribution study, International Journal of Cancer 102 (2002) 469–475.
[29] R.M. Schiffelers, G.A. Koning, T.L.M. ten Hagen, M. Fens, A.J. Schraa, A. Janssen, R.J. Kok, G. Molema, G. Storm, Anti-tumor efficacy of tumor vasculature-targeted liposomal doxorubicin, Journal of Controlled Release 91 (2003) 115–122.